Progress in Oceanography 165 (2018) 110–122

Contents lists available at ScienceDirect

Progress in Oceanography

journal homepage: www.elsevier.com/locate/pocean

# Variability in oceanographic barriers to coral larval dispersal: Do currents shape biodiversity?

D.M. Thompson[a,f,*], J. Kleypas[a], F. Castruccio[a], E.N. Curchitser[b], M.L. Pinsky[c], B. Jönsson[d], J.R. Watson[e]

[a] National Center for Atmospheric Research, P.O. Box 3000, Boulder, CO 80307-3000, United States
[b] Dept. of Environmental Sciences, Rutgers University, 14 College Farm Road, New Brunswick, NJ 08901, United States
[c] Dept. of Ecology, Evolution, and Natural Resources, Rutgers University, 14 College Farm Road, New Brunswick, NJ 08901, United States
[d] Institute for the Study of Earth, Oceans, and Space, University of New Hampshire, 8 College Road, Durham, NH 03824, United States
[e] College of Earth, Ocean and Atmospheric Sciences, Oregon State University, Corvallis 97330, United States
[f] Department of Earth & Environment, Boston University, 685 Commonwealth Ave, Boston, MA 02215 USA

ARTICLE INFO

*Keywords:*
Coral reefs
Larval dispersal
Connectivity
High-resolution modeling
Coral Triangle

ABSTRACT

The global center of marine biodiversity is located in the western tropical Pacific in a region known as the "Coral Triangle" (CT). This region is also considered the most threatened of all coral reef regions, because multiple impacts, including rising temperatures and coral bleaching, have already caused high mortality of reef corals over large portions of the CT. Larval dispersal and recruitment play a critical role in reef recovery after such disturbances, but our understanding of reproductive connectivity between reefs is limited by a paucity of observations. Oceanographic modeling can provide an economical and efficient way to augment our understanding of reef connectivity, particularly over an area as large as the CT, where marine ecosystem management has become a priority. This work combines daily averaged surface current velocity and direction from a Regional Ocean Modeling System developed for the CT region (CT-ROMS) with a Lagrangian particle tracking tool (TRACMASS) to investigate the probability of larval transport between reefs for a typical broadcasting coral. A 47-year historical simulation (1960–2006) was used to analyze the *potential connectivity*, the physical drivers of larval transport, and its variability following bi-annual spawning events in April and September. Potential connectivity between reefs was highly variable from year to year, emphasizing the need for long simulations. The results suggest that although reefs in this region are highly self-seeded, comparatively rare long-distance dispersal events may play a vital role in shaping regional patterns of reef biodiversity and recovery following disturbance. The spatial pattern of coral "subpopulations," which are based on the potential connectivity between reefs, agrees with observed regional-scale patterns of biodiversity, suggesting that the physical barriers to larval dispersal are a first-order driver of coral biodiversity in the CT region. These physical barriers persist through the 21st Century when the model is forced with the Community Earth System Model (CESM) RCP8.5 climate scenario, despite some regional changes in connectivity between reefs.

## 1. Introduction

Larval dispersal modeling has greatly improved our understanding of potential dispersal, typical dispersal distances/scales and connectivity between populations, and locations of key sources or sinks for larvae (e.g., Cowen et al., 2006; Treml et al., 2008; Kool et al., 2011; Foster et al., 2012; Treml and Halpin, 2012). In coral reef research, simulations of larval dispersal and reef connectivity provide testable hypotheses for phylogeographic and genetic studies (Kool et al., 2010, 2011; Gillespie et al., 2012) and may help identify potential targets for marine protected areas (MPAs) to facilitate recovery following disturbance and promote reef resilience (e.g., Fernandes et al., 2012; Treml and Halpin, 2012; Magris et al., 2014).

Most analyses of larval dispersal have focused on spatial patterns (e.g., Kool et al., 2011; Treml and Halpin, 2012), with relatively few studies addressing the variability of these patterns through time (i.e., Treml et al., 2008; Mitarai et al., 2009; Berkley et al., 2010; Watson et al., 2010, 2012; Snyder et al., 2015; Wood et al., 2016). Critically, no studies to date have looked at the impact of *long-term* (interannual to decadal-scale) climate and oceanographic variability on larval

* Corresponding author at: National Center for Atmospheric Research, P.O. Box 3000, Boulder, CO 80307-3000, United States.
*E-mail address:* thompsod@ucar.edu (D.M. Thompson).

https://doi.org/10.1016/j.pocean.2018.05.007
Received 24 May 2017; Received in revised form 1 February 2018; Accepted 25 May 2018
Available online 26 May 2018
0079-6611/ 

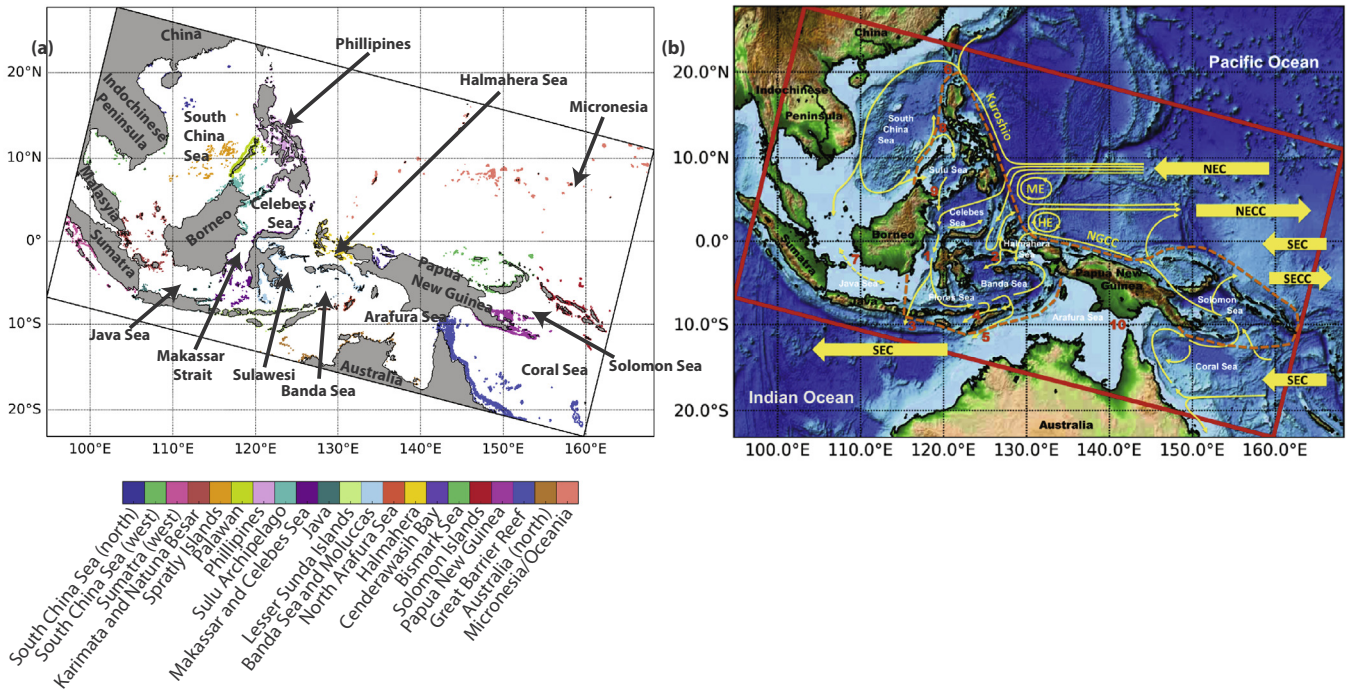


**Fig. 1.** (a) Coral reefs within the CT-ROMS domain (outlined in black), where colors denote the ecoregions defined by Veron et al., (2009). (b) Schematic of ocean circulation in the CT region (Castruccio et al., 2013). Dashed orange line delineates the Coral Triangle (Veron et al., 2009).

dispersal. Identifying how larval dispersal changes across time has therefore been identified as a key research priority (Treml et al., 2015). Such estimates are critical input towards achieving the conservation goals of the Coral Triangle Initiative (CTI, Secretariat, 2009) to preserve reefs in the CT region, as the effectiveness of conservation targets depends in part on whether key sources and sinks of larvae remain stable through time. Because coral larvae drift relatively passively with surface ocean currents, patterns of larval dispersal and reef connectivity will be influenced by both intra- and inter-annual variability in regional climate and ocean currents. For example, the strength of the south equatorial current (SEC) and the Indonesian Throughflow (two major features of surface advection in the CT region) are both affected by the state of the El Niño-Southern Oscillation (ENSO) (e.g., Bray et al., 1996; Gordon and Fine, 1996; Meyers, 1996; Sprintall and Révelard, 2014) and Pacific Decadal Variability (Wainwright et al., 2008; Feng et al., 2011). Seasonal reversal of winds associated with the Asian monsoon system also impact the strength and direction of many of the region's major surface currents (e.g., Wyrtki, 1961; Masumoto and Yamagata, 1991; Han et al., 2009). The locations of the Halmahera and Mindanao Eddies (HE and ME, respectively; Fig. 1) also change between seasons and ENSO phases, shifting southeastward during the boreal winter and during El Niño events (Kashino et al., 2013).

In this study, we take the first look at the stability of connectivity patterns and the location of key source/sink reefs through time in the CT region: from season-to-season and year-to-year and from the historical to future climate states. We investigate the spatial and temporal variability in "potential connectivity" (following Mitarai et al., 2009; Watson et al., 2010, 2012)—the physical drivers of larval dispersal—in the CT (Veron et al., 2009) over a 47-year historical and two 20-year future climate simulations. Although biological factors—e.g., fecundity (Baird and Marshall, 2002; Sudek et al., 2011), precompetency period (Heyward et al., 2002; Figueiredo et al., 2014), survivability (Edmunds et al., 2001; Bassim and Sammarco, 2003; Baums et al., 2006; Nozawa and Harrison, 2007; Randall and Szmant, 2009), and settlement (Coles, 1985)—further modify (and typically reduce) reef connectivity ("realized connectivity"), this approach allows us to isolate the role of physics (e.g., current strength and direction) on connectivity in the region. We focus on the CT region of the western tropical Pacific because it is not only a hotspot for marine biodiversity (Roberts et al., 2002; Hoeksema, 2007), with the greatest numbers species of coral and fish of any region worldwide, but it is also considered one of the most threatened of all reef regions (with hundreds of species on the International Union for Conservation of Nature threatened list) (Roberts et al., 2002; Burke et al., 2006; Carpenter et al., 2008; Burke et al., 2012). Despite the threat to this important biodiversity hotspot, there is still limited coverage of effectively managed MPAs in the CT (~1% of the reef area) (White et al., 2014). The CTI aims to address this issue through improved ecosystem-based management practices, including a network of MPAs to promote ecosystem function and connectivity (e.g., White et al., 2014; Walton et al., 2014).

Motivated by these conservation goals, the present study aims to improve our understanding of spatio-temporal patterns of the physical processes dictating connectivity in the CT (Fig. 1) and how these patterns may change in the future. To this end, we first calculate potential connectivity among reefs in this region and identify key sources and sinks of coral larvae. Larvae from key source reefs have a high probability of reaching other reefs in the region, while key sink reefs are likely to receive larvae from other sites (e.g., Watson et al., 2010). These source and sink reefs may play a critical role in recovery following disturbance. We assess the stability of these patterns over the historical period, by (1) calculating the difference in connectivity patterns between seasons, El Niño/La Niña, and phases of the Pacific Decadal Oscillation (PDO), (2) identifying the dominant spatio-temporal patterns/"modes" of potential connectivity variability and their relation to climate variability (e.g., ENSO, PDO, etc.) and (3) testing the stability of important sources and sinks through time. Such information on the response of larval connectivity to major climate phenomena may improve conservation planning, particularly alongside advances in near-term predictability of climate events and the timing of major phase shifts (Kirtman, 2014; Meehl et al., 2014). We also leverage this long simulation to estimate, for the first time, the length of simulation needed to quantify temporal variability in potential connectivity in this region. Finally, we use future simulations to assess whether the patterns of potential connectivity change under 8.5 $W/m^2$ of climate-change

**Table 1**
*Acropora millepora*: Summary of spawning and larval characteristics.

| Characteristic | Description | References |
|---|---|---|
| Habitat | Shallow reef regions (2–12 m) | Wallace and Willis (2003), IUCN (2015) |
| Distribution | Common throughout the Coral Triangle | Wallace and Richards (2001) |
| Life history strategy | Competitive | Darling et al. (2012) |
| Reproductive mode | Hermaphroditic, broadcast spawner | Wallace and Willis (2003) |
| Spawning period | General: March/April and September/October/November are spawning peaks for most regions in Coral Triangle | Baird et al. (2009) |
| | Palau: *Acropora* sp. spawning observed in late August | Penland et al. (2004) |
| | Malaysia: *A. millepora* spawning observed in April | Chelliah et al. (2015) |
| | Central Great Barrier Reef: *A. millepora* spawning observed in November | Pollock et al. (2017) |
| Larval precompetency | 3 d minimum | Connolly and Baird (2010) |
| Larval competency period | Peaks at around 10 d; mean duration 20 d (95% CI: 16–25 d); max 60 d | Connolly and Baird (2010) |
| Larval survival | > 100 d, but 50% mortality after 14 d | Baird (2001), Connolly and Baird (2010) |

forcing. We end by discussing the implications of this work for future connectivity modeling studies and coral reef conservation.

## 2. Methods

### 2.1. CT-ROMs

We simulate the trajectories of coral larvae using the velocity fields from the Regional Ocean Modeling System developed for the CT region (CT-ROMS; Fig. 1). The CT-ROMS domain spans 95°E–170°E, and 25°S–25°N, with an average spatial resolution of 5 km and 50 vertical levels in terrain-following sigma coordinates. CT-ROMS explicitly solves the tides, and accurately captures regional temperature and circulation patterns (Castruccio et al., 2013). For example, CT-ROMS captures the magnitude and location of major near-surface currents in the region, including the North Equatorial Current (NEC) [and its bifurcation into the northward-flowing Kuroshio and southward-flowing Mindanao currents], North Equatorial Counter Current (NECC), New Guinea Coastal Current (NGCC), and South Equatorial Current (SEC). Importantly, CT-ROMS also captures the region's major eddies (e.g., Mindanao Eddy, Halmahera Eddy), the magnitude and spatial pattern of Eddy Kinetic Energy, and the mean transport through outflow passages of the Indonesian Throughflow over the 2004–2006 period (the observational period of the International Nusantara Stratification and Transport Program) (Castruccio et al., 2013). Finally, correlations between observed and simulated sea level are 0.8–0.95 for all tidal stations, indicating that CT-ROMS captures regional tidal evolution and magnitude (Castruccio et al., 2013).

In addition to capturing the reef-scale circulation features that drive larval transport, the CT-ROMs historical simulation spans 47-years (1960–2006), which permits the first detailed assessment of temporal variability in the physical drivers of reef connectivity. Boundary conditions for this historical simulation were obtained from Simple Ocean Data Assimilation temperature, salinity and velocity (Carton et al., 2000a, 2000b) and Modern Era-Retrospective Analysis for Research Applications (MERRA) reanalysis (Rienecker et al., 2011) air temperature, sea-level pressure, specific humidity, daily short-wave, downwelling longwave, and precipitation. To compare modern and future connectivity patterns in the region, additional CT-ROMS simulations were forced with output from the Community Earth System Model (CESM): 1960–1979 from the 20th Century simulation, and 2040–2059 and 2080–2099 from the 21st Century RCP 8.5 simulation (Hurrell et al., 2013). The RCP 8.5 (Representative Concentration Pathway) climate-change scenario represents the $CO_2$-equivalent greenhouse gas concentration associated with additional radiative forcing of 8.5 W $m^{-2}$ in the year 2100 (Moss et al., 2010).

### 2.2. Potential connectivity

Our approach separates the physical and biological processes of connectivity (following Mitarai et al., 2009; Watson et al., 2010, 2012). Here we present results of the *potential connectivity* between reefs of the CT following biannual (spring and fall) mass spawning events (Penland et al., 2004; Baird et al., 2009; Chelliah et al., 2015; Pollock et al., 2017). Potential connectivity represents the physical drivers of larval dispersal and is calculated as the probability of larval transport between a source reef and a sink reef (Watson et al., 2010). This approach yields a first-order estimate of the degree of connectivity among reefs, and acknowledges that biological processes (e.g., larval mortality) will act to modify (usually reduce) the potential connectivity.

We used the offline particle tracking tool TRACMASS (Döös et al., 2013) to calculate the trajectories of particles representing coral larvae passing through each grid cell of the 5-km resolution CT-ROMS simulation. This offline particle tracking code allows the release and tracking of thousands of particles (larvae), while maintaining high computational efficiency.

Larval spawning, competency, and dispersal are based on the broadcast spawning coral *Acropora millepora* (Table 1). *A. millepora* is common and widespread throughout the CT, and spawns in the spring (March/April) in some regions of the domain, in the fall in others (August/September in Palau & October/November on the Great Barrier Reef), and likely both fall and spring in many others (Table 1). *A. millepora* larvae can become competent to settle within 3 days after spawning, with the largest proportion reaching competency at around 10 days (Connolly and Baird, 2010), after which they can settle out of the water column onto suitable substrates. Although larvae of *A. millepora* can survive more than 100 days (Baird, 2001; Connolly and Baird, 2010), the largest proportion settle between 10 and 30 days post-spawning (Connolly and Baird, 2010). As in previous connectivity modeling studies for broadcast spawning corals (e.g., Wood et al., 2014; Tay et al., 2012), we assume that *A. millepora* larvae behave as passive tracers, since they have very limited ability to swim against horizontal currents and generally only migrate vertically once they are competent to actively explore the substrate for places to settle (e.g., Szmant and Meadows, 2006; Pizarro and Thomason, 2008).

Particles representing coral larvae were released from each 5x5 km grid cell designated as “reef” or “coastal” (Fig. S1). Reef cells were identified based on the IUCN World data base of coral reefs (IMaRS-USF

and IRD, 2005), and "coastal" cells were identified as cells within 2 grid cells of the coastline. Given the computational burden of tracking particles among all reef cells within the CT-ROMS domain, we grouped the reef cells into "reef sites" defined by 8 × 8 (coastal) grid cells (Fig. S1). For each day of a 5-day spawning event, we released 25 particles from each of the oceanic grid cells within a reef site, for a maximum of 8000 particles released from each "reef site" (the exact number of particles released varies with the proportion of oceanic and land cells within the reef site).

We tested a range of particle numbers (between 1 and 50,000 per site (after Simons et al., 2013)) and determined that 8000 particles captured ~95% of the variance in the Lagrangian probability density function (LPDF) observed after a 30-day pelagic larval duration (PLD) (Fig. S2). For this particle sensitivity test, a reference LPDF was calculated by massively seeding particles every day in March 2004 (> 50,000 particles total) for 21 representative reef sites (selected throughout the domain). Particles were then randomly removed from each site, and the LPDF was re-evaluated. The Fraction Unexplained Variance (FUV) statistic (Fig. S2) quantifies the difference between the reference LPDF (all particles) and the LPDF computed with only a portion of the released particles (x axis). The upper bound of the 30-day PLD 95% confidence interval intersects the FUV upper-bound of 5% at ~8000 particles.

Larvae were released at midnight (Babcock et al., 1986) for 5 days surrounding the full moon (Houk and van Woesik pers. communication; Willis et al., 1985, as reviewed by Baird et al. (2009)) closest to April 1 and September 1 (typical spring and fall spawning periods for *A. millepora*, Table 1) of each year over the 1960–2006 historical simulation. Over $1.8 \times 10^7$ larvae were released during each seasonal spawning event, for a total of more than $1.7 \times 10^9$ larvae over all biannual spawning events in the 47 year simulation. We present potential connectivity among reefs following spring and fall spawning as a conservative estimate of connectivity among reefs in this region; key results for individual spawning seasons are also presented in the supplemental information.

Potential connectivity ($C_{ij}$), the probability that a particle from one site (i) reached another site (j) at the end of the PLD, was then calculated for each pair of source and sink sites following the approach of Mitarai et al. (2009). First, the Lagrangian PDF was calculated at the end of the PLD by normalizing the particle density by the total number of particles for each release site. An isotropic Gaussian filter (with a standard deviation of 30 km) was used to spatially filter the discrete Lagrangian PDF (see Mitarai et al., 2009 for more details). Given a 5 km grid size, CT-ROMS captures mesoscale processes on the scale of 50–500 km. As a result, the 30 km filter smooths the grid-scale level noise in the LPDF at without removing any physical features of the ocean circulation. The Lagrangian PDF (LPDF) thus represents the number of particles per $km^2$ at the end of the PLD (either 10 or 30 days following the larval release period) (e.g., see Fig. 2). The only loss of particles is when they exit the domain. Finally, potential connectivity was evaluated from the LPDF for all source and sink reef combinations by multiplying the LPDF by the sink site area to convert the probability densities to probabilities (see Mitarai et al., 2009 for more details). We therefore analyze the connectivity patterns at the end of the PLD only (i.e., larvae do not settle along the way). We performed these calculations for two PLDs – 10 days and 30 days – as the majority of *A. millepora* settlement occurs within the first few weeks of spawning (e.g., Tay et al., 2011; Connolly and Baird, 2010). In reality, many coral species have larvae that settle over a wide range of PLDs from 3 to > 30 days and in rare instances > 100 days. We model 10 and 30 day PLDs, as average and conservative estimates, respectively, of potential connectivity among reefs in the CT based on typical larval pre-competency period and survival for *A. millepora* (Table 1).

We used the potential connectivity to calculate the source and sink strength of each site within the domain. Source strength was calculated as the total probability that larvae released from the site will reach a settlement cell (not including self-seeding), while sink strength was calculated as the total probability that larvae will arrive at a reef from any source location other than itself (after Mitarai et al., 2009; Watson et al., 2010). We also calculated source and sink strengths with self-seeding, but show the results with self-seeding removed to highlight the potential for each reef site to provide or receive larvae following disturbance events (when self seeding may be greatly reduced, (Baird and Marshall, 2002; Sudek et al., 2011)).

### 2.3. 20th Century multidecadal variability

To assess variability in potential connectivity over the 47-year CT-ROMS simulation (1960–2006), we calculated the standard deviation and coefficient of variation in potential connectivity, source strength, and sink strength. We also performed empirical orthogonal function (EOF) analysis on the annual potential connectivity matrix over the entire 47-year span of spring and fall spawning events (i.e., $C_{ij}$, the square matrix of the probability of dispersal between the 2497 source reefs i and 2497 sink reefs j over 94 individual spawning events; dimensions: 2497 × 2497 × 94). This EOF analysis was used to assess the dominant modes of variability in potential connectivity (i.e., patterns of $C_{ij}$ variability across all 94 spawning events) and their relation to major modes of climate variability. To assess the impact of major climate systems on potential connectivity in the region, we calculated the correlation of the top principal components with indices of the El Niño-Southern Oscillation (Niño 3.4 index; (Smith et al., 2008); El Niño modoki index; (Ashok et al., 2007)), Indian Ocean dipole (IOD mode index, (Saji et al., 2005)), and Pacific Decadal Oscillation (PDO index; (Mantua et al., 1997; Zang et al., 1997)). Finally, we also calculated the difference in source strength and sink strength between strong historical El Niño (1965, 1972, 1982, 1997) and La Niña (1973, 1988, 1998, 1999) events and between positive (1977–1997) and negative (1960–1976) phases of the PDO.

### 2.4. 21st Century projection of larval dispersal

To assess whether potential connectivity patterns may change in the future, we tracked particles using the approach described above, but for three 20-year periods of CT-ROMS simulations forced with output from the Community Earth System Model (CESM): 1960–1979 from the 20th Century simulation, and 2040–2059 and 2080–2099 from the 21st Century RCP 8.5 simulation (Hurrell et al., 2013).

### 2.5. Potential connectivity "subpopulations"

We used the potential connectivity matrix to assess temporal variability in metapopulation structure at regional scales within the CT region. Using the methodology of Jacobi et al., (2012), we identified the "subpopulation" structure from the potential connectivity matrix. This method minimizes the mean connectivity among subpopulations (Q) for a given number of subpopulations, defined as the connectivity between subpopulations $\widetilde{C}_{kl}$ normalized against self-recruitment (Eq. (1)); it iteratively identifies groups of sites that are strongly connected to each other, but are only weakly connected to other sites (Jacobi et al., 2012).

$$Q = \langle \widetilde{C}_{kl} / \widetilde{C}_{kk} \rangle_k, \quad \text{where } \widetilde{C}_{kl} = \left\langle \sum_{i \in L_k} C_{ij} \right\rangle_{j \in L_l} \tag{1}$$

is the connectivity matrix between subpopulation k and subpopulation l, $L_k$ denotes the sites in subpopulation k, and $\widetilde{C}_{kk}$ is the self recruitment within a subpopulation. We also tested the sensitivity of the results to the choice of the number of subpopulations retained. This approach allowed us to assess "hard" and "soft" physical barriers to larval dispersal within the region as we increased the number of subpopulations retained: hard barriers between subpopulations remained independent

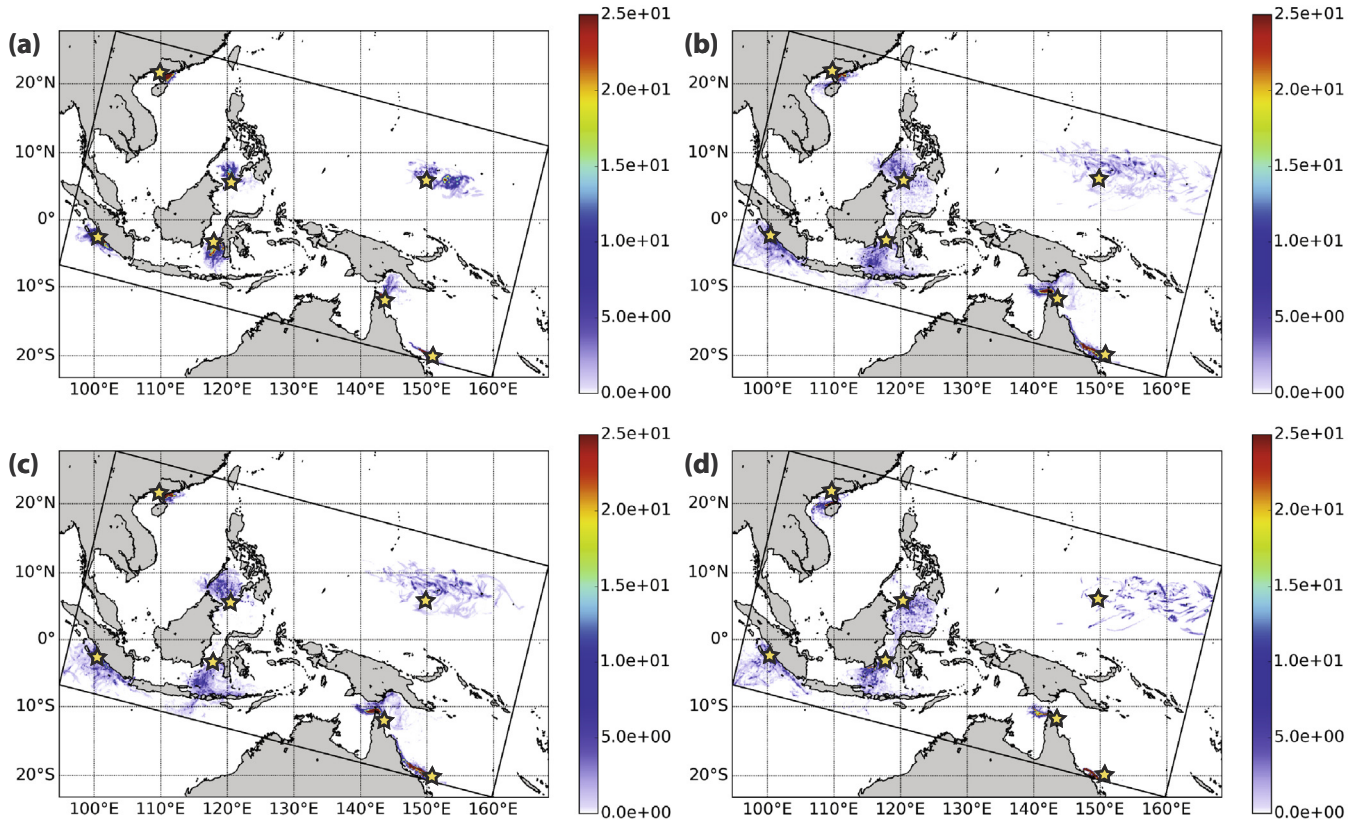


**Fig. 2.** Lagrangian probability density functions (LPDFs) for a subset of 7 larvae release sites (yellow stars) distributed throughout the CT domain for (a) annual spring and fall spawning after a 10-day pelagic larval duration (PLD) and (b) annual spring and fall spawning, (c) spring spawning (d) and fall spawning after a 30-day pelagic larval duration (PLD). All show the average LPDF pattern over the 47-year historical period.

of the number of subpopulations, while soft barriers were observed as additional subpopulations were added and existing subpopulations were subdivided.

## 3. Results

### 3.1. Potential connectivity spatio-temporal patterns

Consistent with previous work, we find that reefs in the CT region are greatly self-seeded (Table 2, Figs. 2, 3), with greater probabilities of self-seeding and short dispersal distances after a 10-day PLD than after a 30-day PLD (Table 2, Figs. S3, S4). With a 10-day PLD, the probability of self-seeding was ~11% on average across the domain, and on some reefs as high as > 99.9%; with a 30-day PLD, the probability of self-seeding was ~5% on average and as high as 57%. Nonetheless, connectivity was also observed across large spatial scales, particularly after a 30-day PLD (Fig. S3). Connectivity was observed within and across ecoregions defined by Veron et al. (2009) (Figs. 1, S4), particularly among reefs within the Banda, Moluccas, Makassar, and Celebes Sea regions (Fig. 1).

Several important source and sink regions (i.e., sites with source/sink strength around 0.6 or greater) were identified in the analysis (Fig. 4). Key source regions of coral larvae included the Great Barrier Reef, west Sumatra, Singapore, Banda and Halmahera Seas, and the (central) Philippines. Key sink regions included the Great Barrier Reef, northern Australia, west Sumatra, Singapore, Banda and Halmahera Seas, Makassar Strait, and the (central) Philippines (note that some regions rank high as both sources and sinks). In contrast, the Coral Sea, Micronesia, and northern South China Sea were much more isolated, with little connectivity to other reefs within the CT.

However, we found that these patterns of potential connectivity within the Coral Triangle were highly variable between seasons and years (Fig. 3). First, the pattern and strength of long distance dispersal varied between the spring and fall, with higher average connectivity

**Table 2**
Potential connectivity statistics, averaged for the 47-year hindcast period.

| | Mean | Max | Min | Std |
|---|---|---|---|---|
| *Spring & fall (30-day PLD)* | | | | |
| Potential connectivity | 1.37E-4 | 0.36 | 0 | 1.87E-3 |
| Source power | 0.40 | 0.88 | 0.001 | 0.16 |
| Sink power | 0.39 | 2.95 | 3.7E-4 | 0.32 |
| Self seeding | 0.019 | 0.36 | 1.26E-11 | 0.034 |
| Percent self seeding | 4.5% | 57% | 2.6E-9% | 7.2% |
| *Spring (30-day PLD)* | | | | |
| Potential connectivity | 1.29E-4 | 0.18 | 0 | 2.82E-3 |
| Source power | 0.38 | 0.89 | 4.75E-5 | 0.16 |
| Sink power | 0.37 | 2.32 | 3.0E-4 | 0.30 |
| Self seeding | 0.014 | 0.176 | 2.39E-11 | 0.02 |
| Percent self seeding | 3.8% | 50.0% | 7.08E-9% | 4.9% |
| *Fall (30-day PLD)* | | | | |
| Potential connectivity | 1.46E-4 | 0.63 | 0 | 1.59E-3 |
| Source power | 0.43 | 0.98 | 1.1E-3 | 0.19 |
| Sink power | 0.42 | 4.83 | 1.01E-11 | 0.47 |
| Self seeding | 0.027 | 0.63 | 6.67E-14 | 0.06 |
| Percent self seeding | 5.7% | 89.6% | 1.77E-11% | 22.5% |
| *Spring & fall (10-day PLD)* | | | | |
| Potential connectivity | 0.0097 | 0.76 | 4.77E-14 | 0.027 |
| Source power | 0.55 | 1.00 | 0.0017 | 0.21 |
| Sink power | 0.53 | 3.88 | 1.83E-7 | 0.39 |
| Self seeding | 0.063 | 0.73 | 4.8E-14 | 0.086 |
| Percent self seeding | 11.3% | 99.99% | 5.5E-12% | 12.9% |

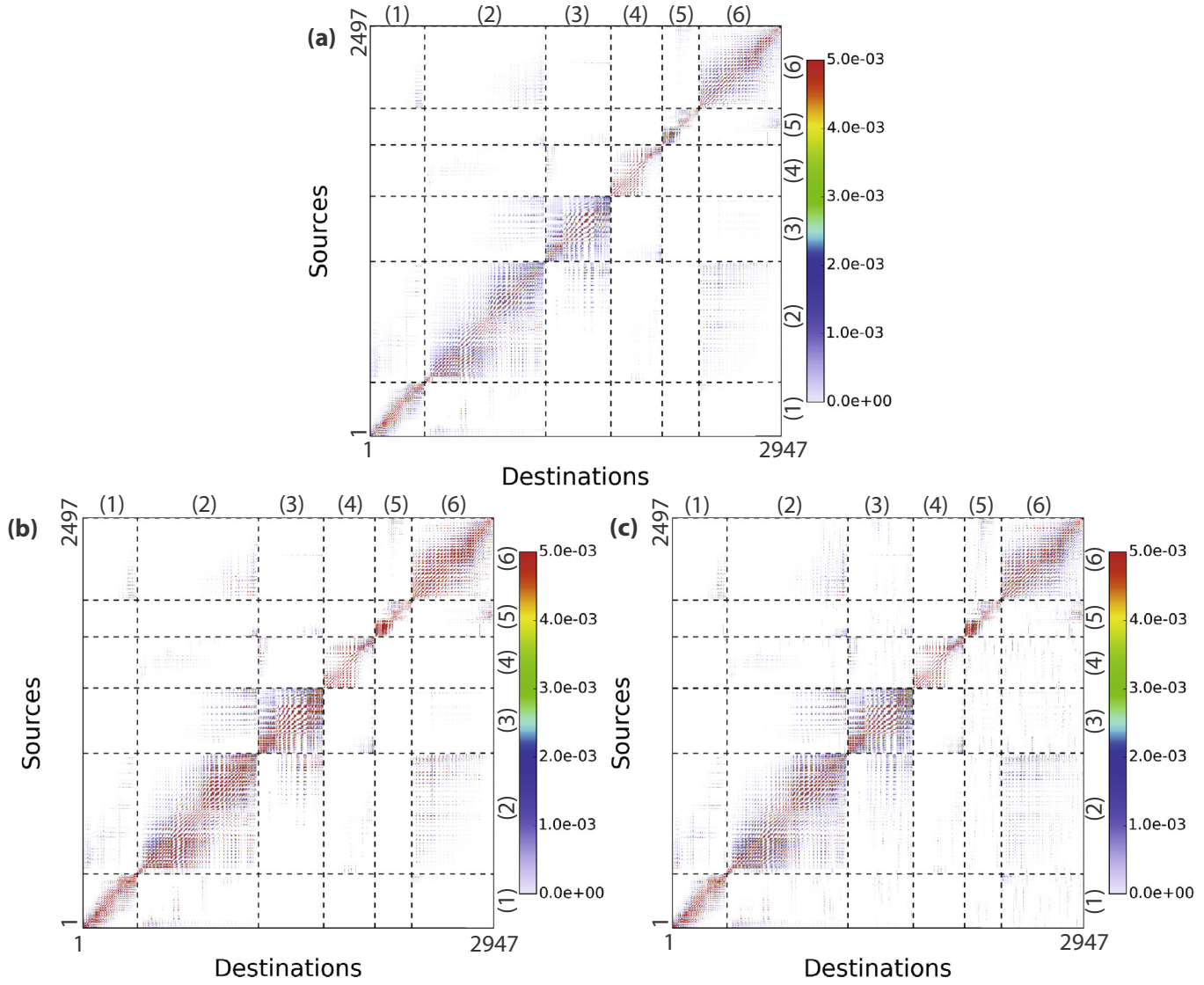


**Fig. 3.** Potential connectivity (i.e. probability of dispersal between site i and j, including self seeding) of *Acropora millepora* larvae in the CT region, calculated based on a 30-day pelagic larval duration following spring and fall spawning over the entire 1960–2006 historical ROMS simulation. (a) Mean potential connectivity over all spring and fall spawning events, (b) standard deviation of potential connectivity over all spring and fall spawning events (depicting seasonal and interannual connectivity variability), and (c) standard deviation of annual average connectivity (interannual connectivity variability). Potential connectivity was calculated from the Lagrangian PDF for all reef release sites (supplemental Fig. 1), with 2497 sources on the y-axis, 2497 sinks on the x-axis, and self-seeding (particles settling within their release location) along the diagonal. Sites are separated (dashed lines) into the 6 main connectivity subpopulations (Fig. 8), noted in parentheses along each secondary axis.

among reefs during the fall spawning events (Table 2). This intra-annual variability in potential connectivity contributed to the high variability in potential connectivity observed between all seasons and years of the simulation (Fig. 3b, Table 2). Nonetheless, the annual average potential connectivity indicates that potential connectivity also varies greatly from year to year, such that the standard deviation in potential connectivity among years was greater than that of the mean at most sites (Fig. 3c). As a result, the strength of source/sink regions also varied greatly from year to year (Table 2, Fig. 4). The difference between strong El Niño (1965, 1972, 1982, 1997) and La Niña (1973, 1988, 1998, 1999) events suggests that the strength of key source and sink regions was reduced slightly overall during El Niño events, although the impact was spatially heterogeneous (i.e., high standard deviation; Table 3, Fig. 5). In contrast, we found little difference or spatial variability in source or sink strength between PDO positive (1977–1997) and PDO negative (1960–1976) states (Table 3, Fig. 5).

EOF analysis of the annual potential connectivity matrix over the full 47-year simulation suggests that year-to-year potential connectivity variability was primarily stochastic, with the top two modes of connectivity variability explaining only about 12% of the variance (Fig. 6). The first principal component (PC1), which explains 6.5% of the variance, was strongly correlated with the ERSSTv3b (Smith et al., 2008) Niño 3.4 index (r = 0.49) and the El Niño Modoki index (Ashok et al., 2007) (r = 0.51). Regression of PC1 on the ROMS SST and surface current velocity and direction fields revealed a pattern consistent with the impact of ENSO in this region (which emerges as the first principle component of both the SST and velocity fields with the same fingerprint). During El Niño or El Niño Modoki events, the south equatorial current is anomalously weak, advection westward into the CT is reduced, and SSTs are anomalously cool throughout the majority of the CT region. The second principal component (PC2) explains 5.3% of the variance and is strongly correlated with the dipole mode index (r = 0.5), an index of the strength of the Indian Ocean dipole (IOD, (Saji et al., 1999)). The impact of the IOD on SST and surface currents is

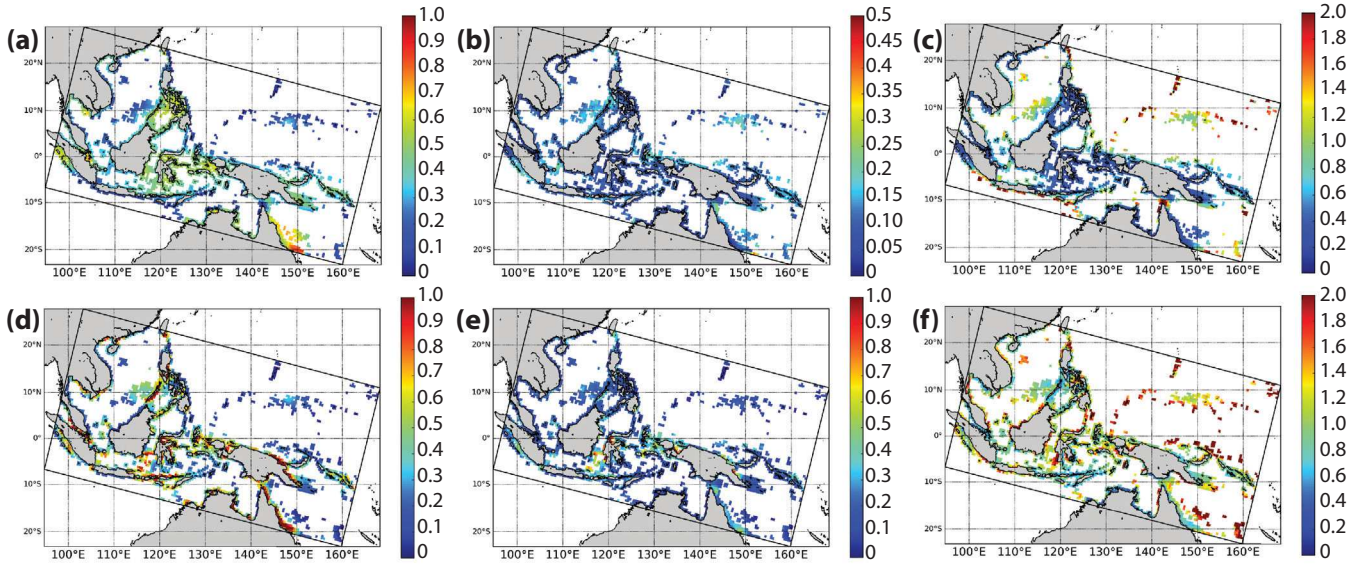


**Fig. 4.** The mean (a, d), standard deviation (b, e), and coefficient of variation (c, f) of source strength (a–c) and sink strength (d–f) for a 30-day PLD following combined (annual average) spring and fall spawning for the 1960–2006 historical simulation (n = 94 spawning events). Source strength is the sum of the probability that particles released from the site successfully reach another settlement site (not including self-seeding) and sink strength is the sum of the probability that particles arrive at a settlement site from any source location but itself.

**Table 3**
Potential connectivity difference statistics between (a) strong historical El Niño (1965, 1972, 1982, 1997) and La Niña (1973, 1988, 1998, 1999) events (El Niño minus La Niña) (b) positive (1977–1997) and negative (1960–1976) phases of the Pacific Decadal Oscillation (PDO) (+PDO minus –PDO), and between (c) the 2080–2100 CESM 8.5 and CESM 1960–2006 hindcast simulations (2080–2100 minus 1960–2006). All statistics are for a 30-day PLD.

| | Mean | Max | Min | Std |
|---|---|---|---|---|
| *(a) El Nino – La Nina* | | | | |
| Potential connectivity | −3.87E-5 | 0.56 | −0.55 | 0.03 |
| Source power | −0.03 | 0.94 | −0.68 | 0.18 |
| Sink power | −0.03 | 7.0 | −3.47 | 0.51 |
| Self seeding | −0.003 | 0.34 | −0.38 | 0.06 |
| *(b) (+)PDO – (−)PDO* | | | | |
| Potential connectivity | −3.13E-5 | 0.30 | −0.19 | 0.005 |
| Source power | −0.004 | 0.39 | −0.40 | 0.06 |
| Sink power | −0.004 | 1.38 | −1.94 | 0.16 |
| Self seeding | 0.0004 | 0.13 | −0.14 | 0.014 |
| *(c) (2080–2100) – (1960–2006)* | | | | |
| Potential connectivity | 5.74E-6 | 0.07 | −0.1 | 0.001 |
| Source power | 0.0007 | 0.15 | −0.56 | 0.044 |
| Sink power | 0.0007 | 0.75 | −0.53 | 0.088 |
| Self seeding | −0.0005 | 0.038 | −0.046 | 0.006 |

similar to that of ENSO in this region, but with lower amplitude changes (Fig. 6). As during El Niño events, the south equatorial current and advection westward weaken during positive IOD events, and SSTs are anomalously cool across much of the region.

Given the high year-to-year variability in potential connectivity within this region, we assessed the number of simulated years needed to capture the magnitude of interannual potential connectivity variability observed over this 47-year simulation. We find that connectivity variability increases with simulation length up until ~20 years, after which the connectivity variability stabilizes at near the mean value for the full 47-year simulation (Fig. 7). These results demonstrate that a simulation of at least 20 years in length is needed to capture > 95% of total (intrannual and interannual) potential connectivity variability (Fig. 7). Further, these results show that simulations less than 10 years in length are likely to grossly underestimate the magnitude of potential connectivity variability and overestimate the stability of source and sink reefs.

### 3.2. Potential connectivity "subpopulations"

In the CT region, the mean connectivity between subpopulations drops off rapidly with less than 10 subpopulations, suggesting that 10 or fewer subpopulations are favored by the surface flow in the region (Fig. S5). To investigate the major physical barriers to larval dispersal (meaning those driven strictly by the physics), we plot the subpopulations over this range, starting with 9 subpopulations and decreasing to 4 subpopulations (Fig. 8). Comparing among these results, we can also identify the strength of each of these barriers: the strongest barrier appears between the first two subpopulations, then the next strongest with 3 subpopulations, etc. With a 30-day PLD, for example, these results suggest that the Malaysian and western Indonesian reefs (subpopulation 1 denoted in yellow, Figs. 8 & S6) are strongly isolated from other reefs in the region. The northern Australia and the Great Barrier Reef (subpopulation 4 denoted in green, Figs. 8 & S6) are strongly isolated from the other reefs in the region, but there are also "softer" barriers between the GBR and the rest of Northern Australia (Figs. 8, S6). Similarly, the northern and southern Philippines and Micronesia (subpopulations 2–2.2 denoted in shades of blue) are weakly isolated from one another, but are strongly isolated from other reefs in the Coral Triangle (Figs. 8, S6). The northern Banda Sea and Halmahera sea/eddy region (subpopulations 3.1 and 3.2 denoted in red/light red) are also weakly isolated from the southern Banda Sea and Makassar straight region (subpopulation 3 denoted in dark red, Figs. 8, S6). Comparison of the subpopulation structure between spring and fall spawning events suggests some of these softer barriers may be attributed to seasonal differences in the strength of these barriers (Fig. S7). While the overall subpopulation structure is similar between seasons, reefs across the Makassar strait (N to S) and between the Halmahera and northern Banda Sea regions are more connected during the fall spawning event than in the spring (Fig. S7). Although these breaks between subpopulations differed between spawning seasons as a function of seasonal current variability (Fig. S7), they were generally insensitive to the pelagic larval duration (Fig. S8).

Regardless of the choice of number of subpopulations (using the Jacobi et al., 2012 method), the mean potential connectivity over the 47-year historical period suggests a subpopulation pattern that broadly resembles the ecoregions of Veron et al. (2009) (Fig. 1a vs Fig. 8).

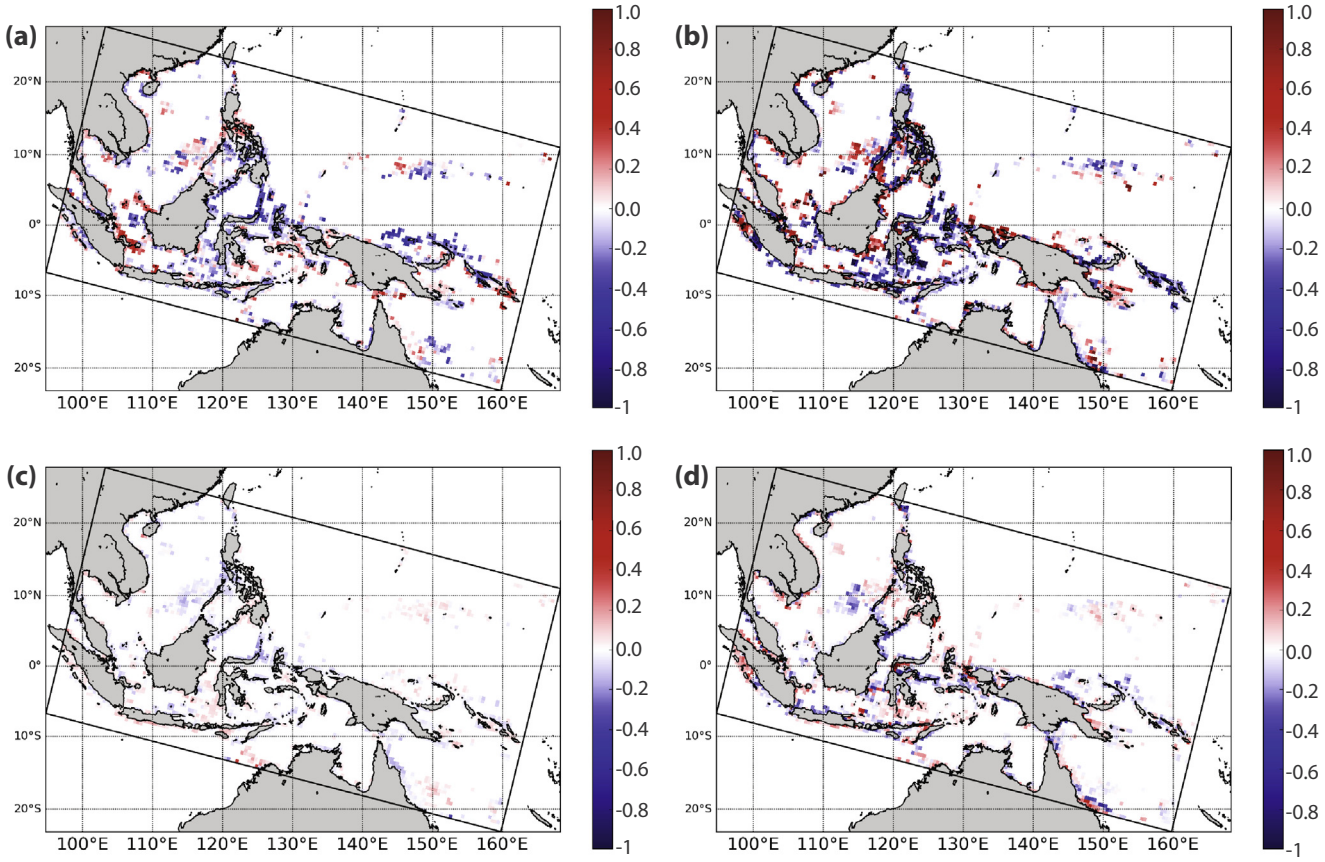


**Fig. 5.** Differences in source strength (a, c) and sink strength (b, d) between strong historical El Niño (1965, 1972, 1982, 1997) and La Niña (1973, 1988, 1998, 1999) events (a, b) and between positive (1977–1997) and negative (1960–1976) phases of the Pacific Decadal Oscillation (PDO) (c, d). Red indicates where warm phase (El Niño/+PDO) conditions result in stronger sources or sinks, and blue where cold phases (La Niña/-PDO) produce stronger sources or sinks.

Furthermore, breaks between subpopulations broadly resemble major phylogenetic breaks (Carpenter et al., 2011a), as well as physical barriers to marine larval dispersal defined by Treml et al. (2015).

### 3.3. Future change in potential connectivity?

The potential connectivity patterns identified in the previous section persisted in the 21st Century simulations under 8.5 $W m^{-2}$ forcing. Although there were some regional differences in source and sink strengths between 1960–1979 and 2080–2099 (Table 3, Fig. 9), the differences were generally very small (and orders of magnitude smaller than mean historical patterns). As a result, the potential connectivity "subpopulations" were largely the same between the historical simulation and the end of the 21st century (Fig. 10). The only exceptions were the reefs along the Makassar straight (eastern coast of Borneo and western coast of Sulawesi), which merged with the subpopulation consisting of the Malaysian and western Borneo reefs. There was no difference in the subpopulation structure between the mid-21st century (2040–2059; results not shown) and the end of the century (2080–2099).

## 4. Discussion

This study offers the first look at potential connectivity variability over the historical period in the Coral Triangle. Our results highlight high intra- and inter-annual potential connectivity variability in this region, with the strength of source/sink regions varying greatly from year to year. We demonstrate that a simulation of at least 20 years in length is needed to capture the magnitude of this variability in connectivity, in contrast to previous connectivity studies in the Coral Triangle that have, owing to computational limitations, understandably examined fewer years (e.g., Treml et al., 2008; Treml and Halpin, 2012; Wood et al., 2014; Wood et al., 2016). The average connectivity pattern across the full 47-year historical period provides additional support for the high probability of self-seeding and short dispersal distances of coral larvae among reefs in the Coral Triangle. The influence of temperature on realized connectivity (not included here) is likely to further modify the probability of long-distance dispersal. The work presented here focuses on the role of physics in larval dispersal within the Coral Triangle (potential connectivity), and may thus be considered a conservative estimate of connectivity in the region. Actual connectivity may be further modified by reproductive output (fecundity), pre-competency period, larval mortality, and settlement and post-settlement mortality, which are in turn a function of temperature, and usually act to reduce connectivity. For example, the probability of larvae seeding from other reefs may increase following a bleaching event, as self-seeding is reduced following local stress and mortality.

### 4.1. Connectivity variability

Potential connectivity in the CT displays strong intra-annual variability, with higher connectivity during the fall mass spawning events. These differences may be attributed to stronger flow in the SEC and channels of the Indonesian throughflow in the fall (September) spawning period relative to the spring (April) spawning period (Fig. S11). Previous observational and modeling studies highlight similarly strong intra-annual variability in the Indonesian throughflow linked to seasonal wind variability, with maximum transport in June–August during the southeast monsoon (Masumoto and Yamagata, 1996; Sprintall et al., 2009). Modeling studies suggest that flow through the

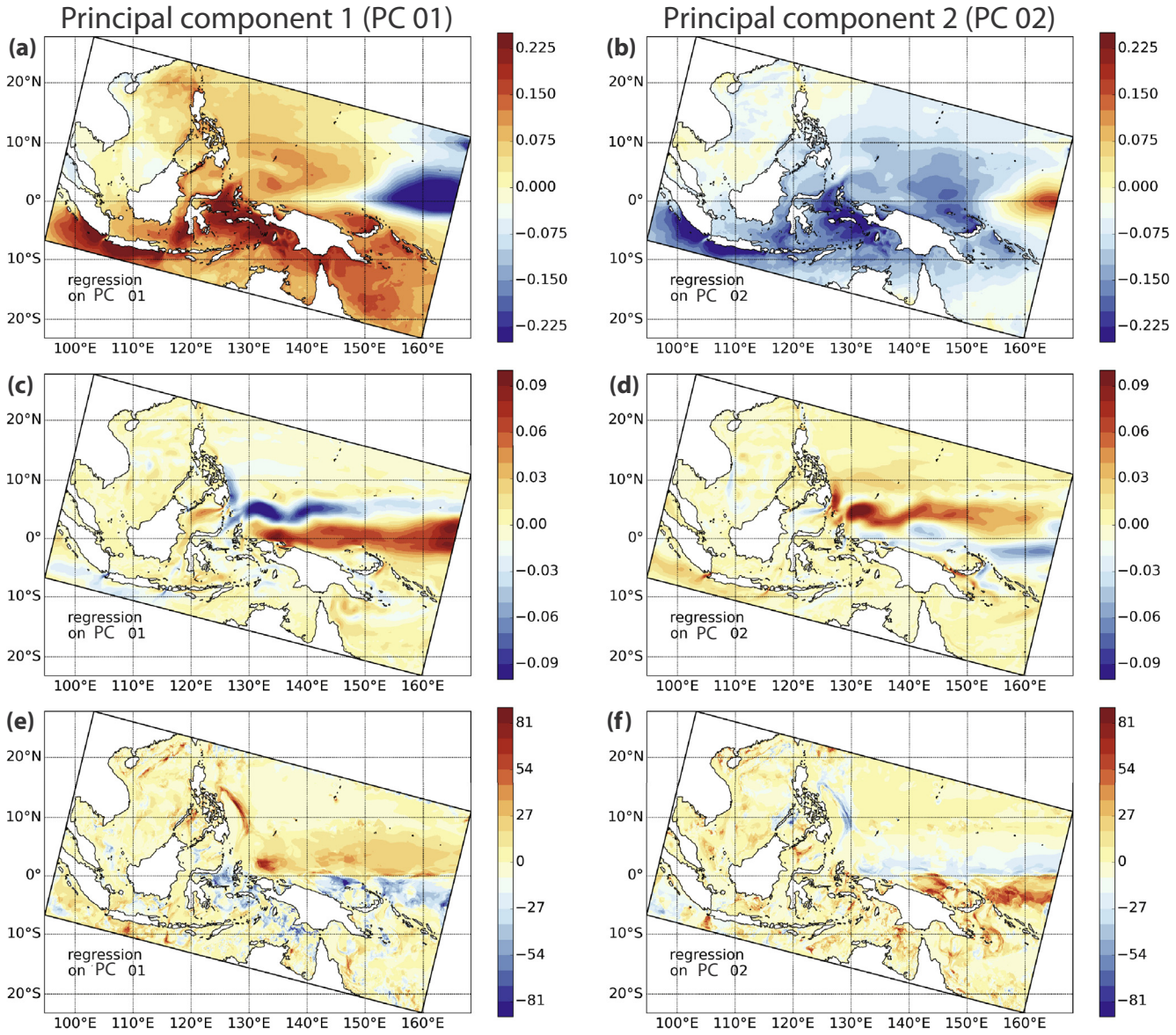


**Fig. 6.** The two dominant modes of potential connectivity variability, explaining ~12% of the variance. Regression of the top two principal components on (a, b) ROMS sea-surface temperature, (c, d) Magnitude of ROMS surface current velocity (m/s, a function of zonal U & meridional V transport), and (e, f) ROMS surface current direction. Panels on the left (a, c, e) depict the regressions for the top principal component (PC 01), and panels on the right (b, d, f) depict regressions for the second principal component (PC 02).

Lombok throughflow region varies in response to wind strength over the equatorial Pacific and Indian Oceans, while flow through the Timor Sea varies in response to winds over southwestern Australia associated with the austral monsoon (Masumoto and Yamagata, 1996).

Interannual potential connectivity variability in this region is primarily driven by year-to-year spatially heterogeneous variability in surface currents, as the top two modes of potential connectivity only explain about 12% of the variance (Fig. 6). This high variability of potential connectivity is consistent with the idea proposed by Van Woesik (2009) that corals spawn in the spring and fall to capitalize on surface wind doldrums, which increases the probability of fertilization and retention of coral larvae (and may thus serve as the ultimate cue for spawning). Similarly, Byers and Pringle (2006) demonstrate that for benthic spawning organisms in the California Current, larvae are more likely to be retained during months when currents are weak and highly variable. However, surface currents during the spring and fall spawning months (April and September) are only slightly weaker overall (mean difference = –0.004) and are also slightly less variable overall (mean std difference = –0.006) than during other months of the year. Ongoing work will investigate monthly connectivity patterns to assess the link between seasonal current stochasticity and reef connectivity to test the hypothesis that seasonal wind doldrums and current variability may serve as an ultimate cue to coral spawning in the CT region by increasing the probability of larval retention and self-seeding.

Potential connectivity variability in this region is also driven by interannual current variability associated with ENSO and the IOD. During positive phases of ENSO and the IOD, the SEC and IT weaken (e.g., Bray et al., 1996; Gordon and Fine, 1996; Meyers, 1996). As a result, reefs in the Indonesian archipelago are stronger sinks of larvae during La Niña events when the SEC and IT are stronger. However, the overall current velocity and larval transport across the entire region are slightly stronger on average during El Niño events (mean difference of 0.004), resulting in a slight decrease in self-seeding (mean probability of self seeding: El Niño = 0.024; La Niña = 0.026), and a change in the

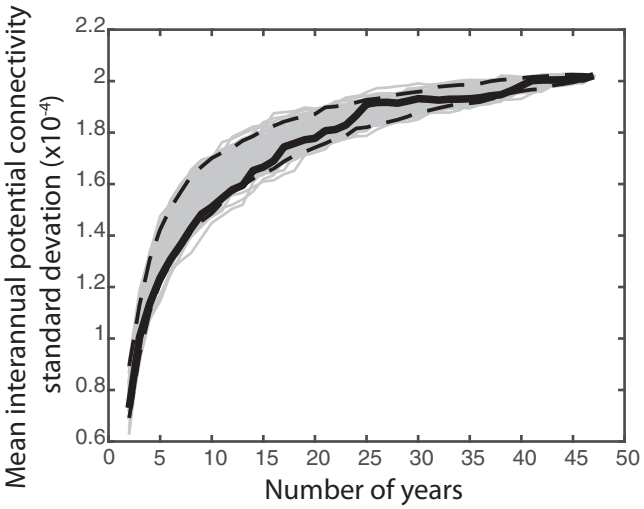


**Fig. 7.** Mean interannual potential connectivity standard deviation (the average standard deviation of annual average potential connectivity across all source/sink site combinations) as a function of the number of years over which potential connectivity was simulated (black). Black dashed lines indicate the 5 and 95% confidence intervals from 100 realizations (gray), where the (annual) temporal evolution of was randomly sampled from the potential connectivity simulation.

spatial pattern of key source and sink reefs in the region. In contrast, the PDO has little impact on potential connectivity, which likely reflects the very minor changes in current velocity ($-0.01\ m\ s^{-1}$) and direction (3.1°) between positive and negative phases of the PDO, respectively, in the CT domain.

Further, source and sink strength are temporally autocorrelated across seasons and years for most reef sites in this region (Figs. S9 & S10, Table S1; mean lag 1 autocorrelation coefficient, AR1, of 0.13 and 0.15 for source and sink strength, respectively), indicating that connectivity patterns are likely to persist across many spawning seasons and years (potentially isolating source and/or sink sites). Source and sink strength display significant autocorrelation at reefs in northern Australia, across the Great Barrier Reef and the Java Sea (max source AR1 = 0.82 and sink AR1 = 0.86). Mean source strength autocorrelation across the CT region remains positive out to a lag of 10 spawning seasons (Table S1), indicating that reefs remain strong or weak sources of larvae for up to 5 years. More critically, sink strength displays positive autocorrelation for over 19 spawning seasons, suggesting that reefs may be cut off from larval supply for over 10 years. This (low-frequency) temporal variability in the strength of key source and sink reefs may therefore delay recovery following disturbance and provide a challenge to identifying conservations targets to promote recovery following disturbance (one of the principle aims of connectivity modeling (e.g., Treml and Halpin, 2012; Magris et al., 2014)).

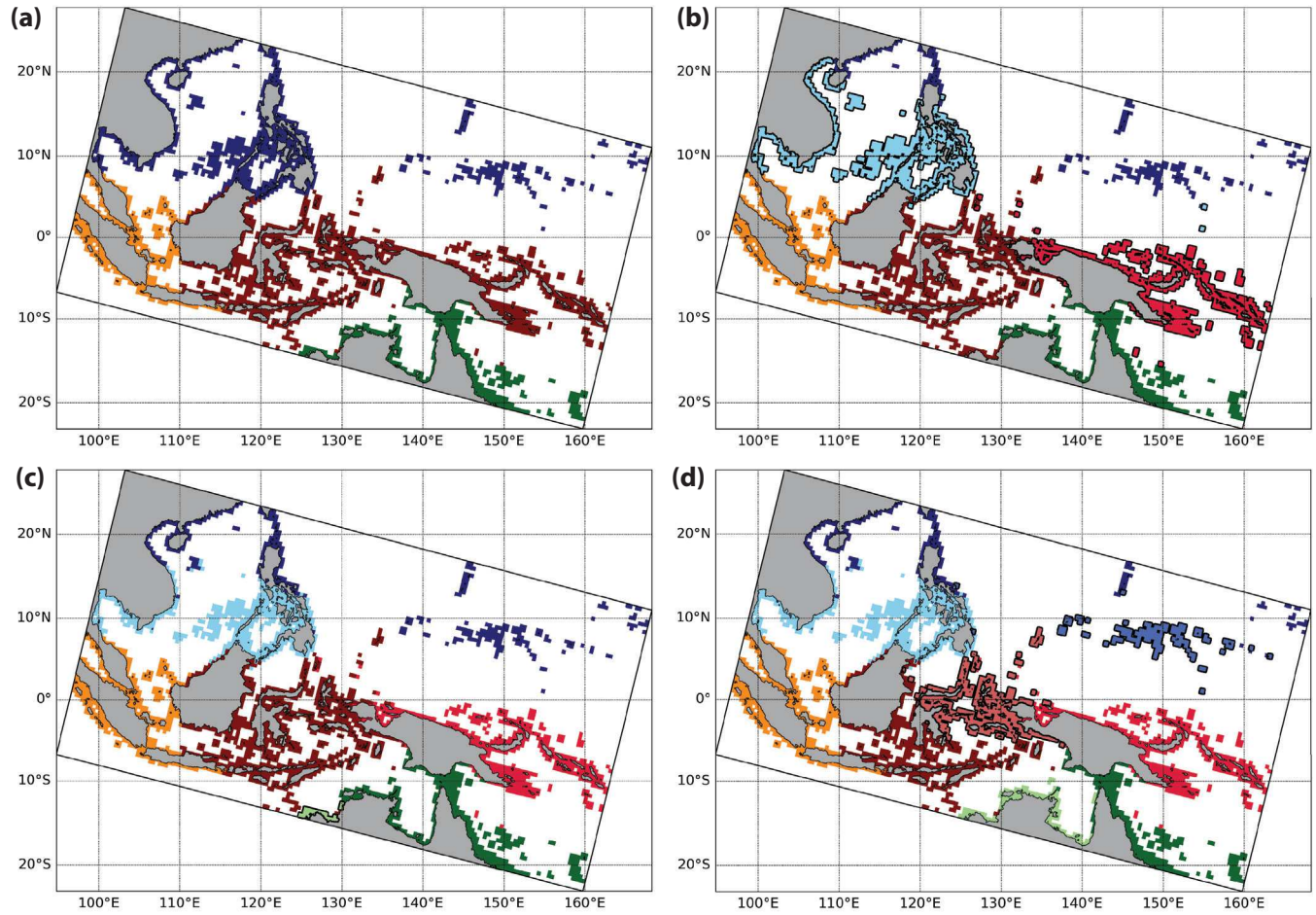


**Fig. 8.** Coral subpopulations determined from potential connectivity for a 30-day PLD of combined spring and fall spawning events (using methodology of Jacobi et al., 2012): (a) 4 subpopulations (mean connectivity between subpopulations, Q = 0.74), (b) 6 subpopulations (Q = 0.83), (c) 7 subpopulations (Q = 0.85), and (d) 9 subpopulations (Q = 0.88). New subpopulations added each iteration are outlined in black.

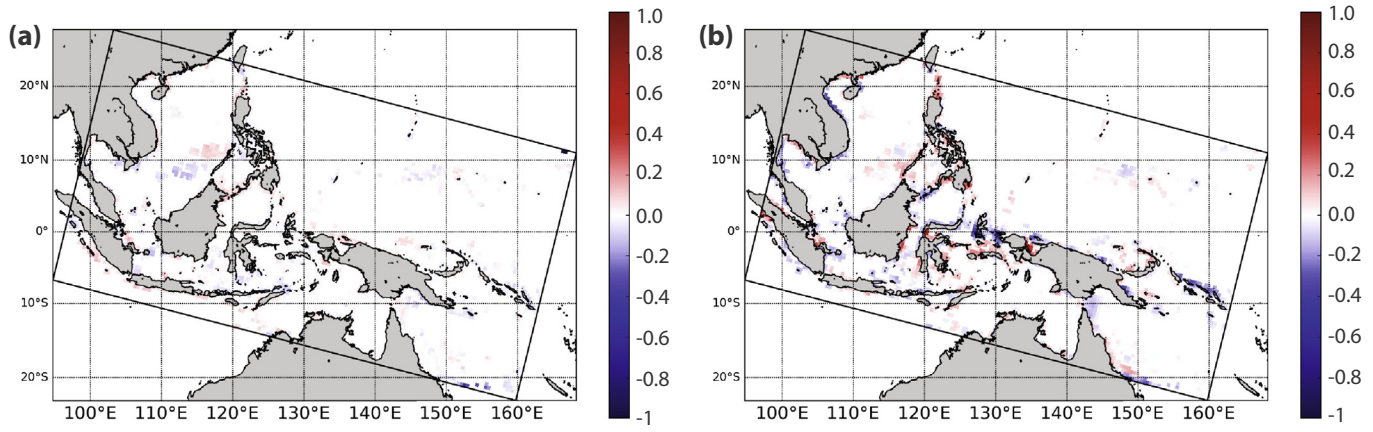


**Fig. 9.** Differences in source strength (a) and sink strength (b) between the CESM 20th century (1960–1979) and RCP 8.5 future scenarios (2080–2099) after a 30-day PLD. Red indicates where sources or sinks strengthen in the future (i.e., stronger in 2080–2099 than in 1960–1979), and blue where the sources or sinks weaken in the future (i.e., weaker in 2080–2099 than in 1960–1979).

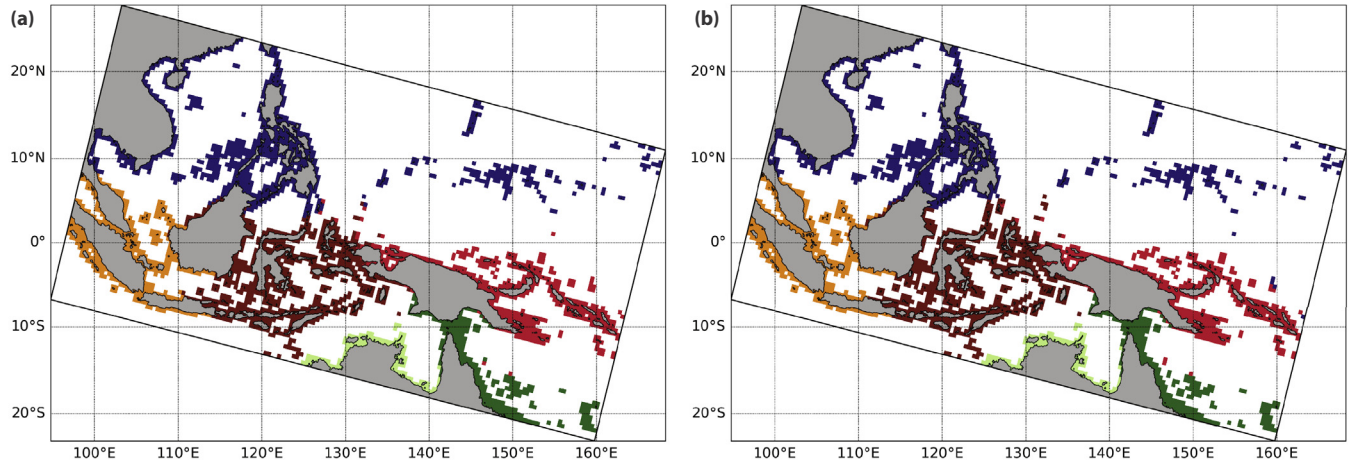


**Fig. 10.** Potential connectivity subpopulations (n = 6) for (a) 1960–1979 (CESM historical, Q = 0.83), and (b) 2080–2099 (CESM RCP 8.5, Q = 0.83), based on spring and fall spawning and a 30-day PLD.

### *4.2. Connectivity subpopulations*

Potential connectivity patterns across the 47-year historical period suggest that physical barriers to dispersal play an important role in shaping patterns of biodiversity. We find that "subpopulations" defined by potential connectivity are broadly similar to the ecoregions of Veron et al. (2009), major phylogenetic lines (Carpenter et al., 2011a) and physical barriers to marine larval dispersal (Treml et al., 2015) in the CT region. In particular, barriers/breaks between the eastern Java Sea and Makassar Straight, northern and southern Philippines, and Molucca Sea and Halmahera Eddy regions are consistent across these studies. However, the previously identified break across the Java Sea, separating Java and Sumatra from Malaysia and the South China Sea (Veron et al., 2009; Carpenter et al., 2011b), was not observed in the potential connectivity subpopulations reported here.

### *4.3. Implications for the future*

Our results suggest that these connectivity patterns persist into the future under 8.5 W $m^{-2}$ of forcing. Although there are some small reef-scale differences in source and sink strength between the 20th century and future climate scenarios, the regional patterns and major physical barriers to larval dispersal remain unchanged. This result suggests that once properly quantified and constrained, historical connectivity patterns and variability may be used to identify conservation targets to promote future recovery and resilience of reefs in the Coral Triangle. Our results emphasize the importance of identifying conservation targets (a) that are *consistently* important sources and sinks for larvae among years of a 20+ year connectivity simulation, such as the one analyzed here, and (b) whose importance as a source/sink is not expected to diminish into the future in response to realistic scenarios of future climate evolution. These criteria may be used along with other commonly used metrics (reef cover, complexity, diversity, etc.) to prioritize candidate conservation targets and promote long-term resilience of coral reefs in the Coral Triangle.

## Acknowledgments

We thank the Advanced Study Program (ASP) Postdoctoral Fellowship Program at the National Center for Atmospheric Research for funding and computational support during D. Thompson's ASP postdoctoral fellowship. Computational resources were provided by NSF-MRI Grant CNS-0821794, the MRI-Consortium: Acquisition of a Supercomputer by the Front Range Computing Consortium (FRCC), and on Yellowstone (ark:/85065/d7wd3xhc) by NCAR's Computational and Information Systems Laboratory. Additional support was provided by Rutgers University and by the National Center for Atmospheric Research, which is sponsored by NSF.

## Appendix A. Supplementary material

Supplementary data associated with this article can be found, in the online version, at https://doi.org/10.1016/j.pocean.2018.05.007.

## References


Ashok, K., Behera, S.K., Rao, S.A., Weng, H., Yamagata, T., 2007. El Niño Modoki and its possible teleconnection. J. Geophys. Res. 112 (C11), C11007. http://dx.doi.org/10.1029/2006JC003798.

Babcock, R.C., Bull, G.D., Harrison, P.L., Heyward, A.J., Oliver, J.K., Wallace, C.C., Willis, B.L., 1986. Synchronous spawnings of 105 scleractinian coral species on the Great Barrier Reef. Mar Biol 90 (3), 379–394. http://dx.doi.org/10.1007/BF00428562.

Baird, A.H., 2001. The Ecology of Coral Larvae: Settlement Patterns, Habitat Selection and the Length of the Larval Phase.

Baird, A.H., Marshall, P.A., 2002. Mortality, growth and reproduction in scleractinian corals following bleaching on the Great Barrier Reef. JSTOR. http://dx.doi.org/10.2307/24866310.

Baird, A.H., Guest, J.R., Willis, B.L., 2009. Systematic and biogeographical patterns in the reproductive biology of scleractinian corals. Ann. Rev. Ecol., Evol. Systemat. 40 (1), 551–571. http://dx.doi.org/10.1146/annurev.ecolsys.110308.120220.

Bassim, K., Sammarco, P., 2003. Effects of temperature and ammonium on larval development and survivorship in a scleractinian coral (< Emphasis Type="Italic" > Diploria < /Emphasis > < Emphasis Type="Italic" > strigosa < /Emphasis >). Mar. Biol. 142 (2), 241–252. http://dx.doi.org/10.1007/s00227-002-0953-z.

Baums, I.B., Paris, C.B., Cherubin, L., 2006. A bio-Oceanographic Filter to Larval Dispersal in a Reef-Building Coral. Limnol Oceanogr, Limnol. Oceanogr.

Berkley, H.A., Kendall, B.E., Mitarai, S., Siegel, D.A., 2010. Turbulent dispersal promotes species coexistence. Ecol. Lett. 13 (3), 360–371. http://dx.doi.org/10.1111/j.1461-0248.2009.01427.x.

Bray, N.A., Hautala, S., Chong, J., Pariwono, J., 1996. Large-scale sea level, thermocline, and wind variations in the Indonesian throughflow region. J. Geophys. Res.: Atmos. 101 (C5), 12239–12254. http://dx.doi.org/10.1029/96JC00080.

Burke, L.M., Reytar, K., Spalding, M., Perry, A., 2012. Reefs at Risk Revisited in the Coral Triangle.

Burke, L., Selig, E., Spalding, M., 2006. In: Reefs at Risk in Southeast Asia, http://dx.doi.org/10.1234/12345678.

Byers, J.E., Pringle, J.M., 2006. Going against the flow: retention, range limits and invasions in advective environments. Mar. Ecol. Prog. Ser. 313, 27–41. http://dx.doi.org/10.3354/meps313027.

Carpenter, K.E., et al., 2008. One-third of reef-building corals face elevated extinction risk from climate change and local impacts. Science 321 (5888), 560–563. http://dx.doi.org/10.1126/science.1159196.

Carpenter, K.E., et al., 2011a. Comparative phylogeography of the coral triangle and implications for marine management, J. Mar. Biol., 2011(2), 1–14, http://doi.org/10.1155/2011/396982.

Carpenter, K.E., et al., 2011b. Comparative phylogeography of the Coral Triangle and implications for marine management, J. Mar. Biol. 2011(2), 1–14, http://doi.org/10.1155/2011/396982.

Carton, J.A., Giese, B., Chepurin, G., Cao, X., 2000a. A Simple ocean data assimilation analysis of the global upper ocean 1950–95. Part I: Methodology, http://dx.doi.org/10.1175/1520-0485(2000)030%3C0294:ASODAA%3E2.0.CO;2, 30(2), 294–309.

Carton, J.A., Chepurin, G., Cao, X., Carton, J.A., Chepurin, G., Cao, X., 2000b. A simple ocean data assimilation analysis of the Global Upper Ocean 1950–95. Part II: Results, 30(2), 311–326, http://doi.org/10.1175/1520-0485(2000)030<0311:ASODAA>2.0.CO;2.

Castruccio, F.S., Curchitser, E.N., Kleypas, J.A., 2013. A model for quantifying oceanic transport and mesoscale variability in the Coral Triangle of the Indonesian/Philippines Archipelago. J. Geophys. Res. Oceans 118 (11), 6123–6144. http://dx.doi.org/10.1002/2013JC009196.

Chelliah, A., Amar, H.B., Hyde, J., Yewdall, K., Steinberg, P.D., Guest, J.R., 2015. First record of multi-species synchronous coral spawning from Malaysia. PeerJ 3 (5876), e777. http://dx.doi.org/10.7717/peerj.777.

Coles, S.L., 1985. In: The Effects of Elevated Temperature on Reef Coral Planula Settlement as Related to Power Station Entrainment, pp. 171–176.

Connolly, S.R., Baird, A.H., 2010. Estimating dispersal potential for marine larvae: dynamic models applied to scleractinian corals. Ecology 91 (12), 3572–3583. http://dx.doi.org/10.1890/10-0143.1.

Cowen, R.K., Paris, C.B., Srinivasan, A., 2006. Scaling of connectivity in marine populations. Science 311 (5760), 522–527. http://dx.doi.org/10.1126/science.1122039.

Darling, E.S., Alvarez-Filip, L., Oliver, T.A., McClanahan, T.R., Côté, I.M., 2012. Evaluating life-history strategies of reef corals from species traits, edited by D. Bellwood. Ecol. Lett. 15 (12), 1378–1386. http://dx.doi.org/10.1111/j.1461-0248.2012.01861.x.

Döös, K., Kjellsson, J., Jönsson, B., 2013. TRACMASS—A Lagrangian trajectory model. In: Preventive Methods for Coastal Protection. Springer International Publishing, Heidelberg, pp. 225–249.

Edmunds, P., Gates, R., Gleason, D., 2001. The biology of larvae from the reef coral < Emphasis Type="Italic" > Porites < /Emphasis > < Emphasis Type="Italic" > astreoides < /Emphasis >, and their response to temperature disturbances. Mar. Biol. 139 (5), 981–989. http://dx.doi.org/10.1007/s002270100634.

Feng, M., Böning, C., Biastoch, A., Behrens, E., Weller, E., Masumoto, Y., 2011. The reversal of the multi-decadal trends of the equatorial Pacific easterly winds, and the Indonesian Throughflow and Leeuwin Current transports, Geophys. Res. Lett. 38(11), n/a–n/a, http://doi.org/10.1029/2011GL047291.

Fernandes, L., Green, A., Tanzer, J., White, A., 2012. Biophysical principles for designing resilient networks of marine protected areas to integrate fisheries, biodiversity and climate change objectives in the Coral ..., Report prepared by The Nature Conservancy for the Coral Triangle Support Partnership.

Figueiredo, J., Baird, A.H., Harii, S., Connolly, S.R., 2014. Increased local retention of reef coral larvae as a result of ocean warming. Nat. Clim. Change 4 (6), 498–502. http://dx.doi.org/10.1038/nclimate2210.

Foster, N.L., et al., 2012. Connectivity of Caribbean coral populations: complementary insights from empirical and modelled gene flow. Mol. Ecol. 21 (5), 1143–1157. http://dx.doi.org/10.1111/j.1365-294X.2012.05455.x.

Gillespie, R.G., Baldwin, B.G., Waters, J.M., Fraser, C.I., Nikula, R., Roderick, G.K., 2012. Long-distance dispersal: a framework for hypothesis testing. Trends Ecol. Evol. 27 (1), 47–56. http://dx.doi.org/10.1016/j.tree.2011.08.009.

Gordon, A.L., Fine, R.A., 1996. Pathways of water between the Pacific and Indian oceans in the Indonesian seas. Nature 379 (6561), 146.

Han, W., Moore, A.M., Levin, J., Zhang, B., Arango, H.G., Curchitser, E., Di Lorenzo, E., Gordon, A.L., Lin, J., 2009. Seasonal surface ocean circulation and dynamics in the Philippine Archipelago region during 2004–2008. Dyn. Atmos. Oceans 47 (1–3), 114–137. http://dx.doi.org/10.1016/j.dynatmoce.2008.10.007.

Heyward, A.J., Smith, L.D., Rees, M., Field, S.N., 2002. Enhancement of coral recruitment by in situ mass culture of coral larvae. Mar. Ecol. Prog. Ser. 230, 113–118. http://dx.doi.org/10.3354/meps230113.

Hoeksema, B.W., 2007. Delineation of the Indo-Malayan centre of maximum marine biodiversity: the coral triangle. In: Biogeography, Time, and Place: Distributions, Barriers, and Islands, vol. 29. Springer, Netherlands, Dordrecht, pp. 117–178.

Hurrell, J.W., et al., 2013. The Community Earth System Model: A Framework for Collaborative Research. American Meteorological Society.

IUCN, 2015. Acropora millepora: Richards, Z.T., Delbeek, J.T., Lovell, E.R., Bass, D., Aeby, G. & Reboton, C., http://doi.org/10.2305/IUCN.UK.2014-1.RLTS.T133666A54304631.en.

IMaRS-USF (Institute for Marine Remote Sensing-University of South Florida), and IRD (Institut de Recherche pour le Developpement), 2005: Millennium Coral Reef Mapping Project. Validated maps., UNEP World Conservation Monitoring Centre, Ed.

Jacobi, M.N., André, C., Döös, K., Jonsson, P.R., 2012. Identification of subpopulations from connectivity matrices. Ecography 35 (11), 1004–1016. http://dx.doi.org/10.1111/j.1600-0587.2012.07281.x.

Kashino, Y., Atmadipoera, A., Kuroda, Y., 2013. Observed features of the Halmahera and Mindanao Eddies. J. Geophys. Res. Oceans 118 (12), 6543–6560. http://dx.doi.org/10.1002/2013JC009207.

Kirtman, B., 2014. Current status of ENSO prediction and predictability, US CLIVAR.

Kool, J.T., Paris, C.B., Barber, P.H., Cowen, R.K., 2011. Connectivity and the development of population genetic structure in Indo-West Pacific coral reef communities. Glob. Ecol. Biogeogr. 20 (5), 695–706. http://dx.doi.org/10.1111/j.1466-8238.2010.00637.x.

Kool, J.T., Paris, C.B., Andréfouët, S., Cowen, R.K., 2010. Complex migration and the development of genetic structure in subdivided populations: an example from Caribbean coral reef ecosystems. Ecography 33 (3), 597–606. http://dx.doi.org/10.1111/j.1600-0587.2009.06012.x.

Magris, R.A., Pressey, R.L., Weeks, R., Ban, N.C., 2014. Integrating connectivity and climate change into marine conservation planning, Biol. Conserv. 170(C), 207–221, http://doi.org/10.1016/j.biocon.2013.12.032.

Mantua, N.J., Hare, S.R., Zhang, Y., Wallace, J.M., Francis, R.C., 1997. A Pacific Interdecadal climate oscillation with impacts on salmon production. Bull. Am. Meteorol. Soc. 78 (6), 1069–1079. http://dx.doi.org/10.1175/1520-0477(1997)078<1069:APICOW>2.0.CO;2.

Masumoto, Y., Yamagata, T., 1991. Response of the Western Tropical Pacific to the Asian Winter Monsoon: the generation of the Mindanao Dome. J. Phys. Oceanogr. 21 (9), 1386–1398. http://dx.doi.org/10.1175/1520-0485(1991) 021<1386:ROTWTP>2.0.CO;2.

Masumoto, Y., Yamagata, T., 1996. Seasonal variations of the Indonesian throughflow in a general ocean circulation model. J. Geophys. Res. 101 (C5), 12287–12293. http://dx.doi.org/10.1029/95JC03870.

Meehl, G.A., et al., 2014. Decadal Climate Prediction: An Update from the Trenches. Bull. Am. Meteorol. Soc. 95 (2), 243–267. http://dx.doi.org/10.1175/BAMS-D-12-00241.1.

Meyers, G., 1996. Variation of Indonesian throughflow and the El Niño-Southern Oscillation. J. Geophys. Res.: Atmos. 101 (C5), 12255–12263. http://dx.doi.org/10.1029/95JC03729.

Mitarai, S., Siegel, D.A., Watson, J.R., Dong, C., McWilliams, J.C., 2009. Quantifying connectivity in the coastal ocean with application to the Southern California Bight. J. Geophys. Res. 114 (C10), C10026–C10121. http://dx.doi.org/10.1029/2008JC005166.

Moss, R.H., et al., 2010. The next generation of scenarios for climate change research and assessment. Nature 463 (7282), 747–756. http://dx.doi.org/10.1038/nature08823.

Nozawa, Y., Harrison, P.L., 2007. Effects of elevated temperature on larval settlement and post-settlement survival in scleractinian corals, < Emphasis Type="Italic" > Acropora solitaryensis < /Emphasis > and < Emphasis Type="Italic" > Favites chinensis < /Emphasis > Mar. Biol. 152 (5), 1181–1185. http://dx.doi.org/10.1007/s00227-007-0765-2.

Penland, L., Kloulechad, J., Idip, D., Van Woesik, R., 2004. Coral spawning in the western Pacific Ocean is related to solar insolation: evidence of multiple spawning events in Palau. Coral Reefs 23 (1), 133–140. http://dx.doi.org/10.1007/s00338-003-0362-x.

Pizarro, V., Thomason, J.C., 2008. How do swimming ability and behaviour affect the dispersal of coral larvae. In: Proceedings of the 11th International Coral Reef

Symposium, Fort Lauderdale, Florida, vol. 1, pp. 464–467.
Pollock, F.J., et al., 2017. Coral larvae for restoration and research: a large-scale method for rearing Acropora milleporalarvae, inducing settlement, and establishing symbiosis. PeerJ 5 (2), e3732. http://dx.doi.org/10.7717/peerj.3732.
Randall, C.J., Szmant, A.M., 2009. Elevated temperature reduces survivorship and settlement of the larvae of the Caribbean scleractinian coral, < Emphasis Type = "Italic" > Favia fragum < /Emphasis > (Esper). Coral Reefs 28 (2), 537–545. http://dx.doi.org/10.1007/s00338-009-0482-z.
Rienecker, M.M., et al., 2011. MERRA: NASA's modern-era retrospective analysis for research and applications, 24(14), 3624–3648, http://doi.org/10.1175/JCLI-D-11-00015.1.
Roberts, C.M., et al., 2002. Marine biodiversity hotspots and conservation priorities for tropical reefs. Science 295 (5558), 1280–1284. http://dx.doi.org/10.1126/science.1067728.
Saji, N.H., Goswami, B.N., Vinayachandran, P.N., Yamagata, T., 1999. A dipole mode in the tropical Indian Ocean. Nature 401 (6751), 360–363. http://dx.doi.org/10.1038/43854.
Saji, N.H., Ambrizzi, T., Ferraz, S.E.T., 2005. Indian Ocean dipole mode events and austral surface air temperature anomalies. Dyn. Atmos. Oceans 39 (1–2), 87–101. http://dx.doi.org/10.1016/j.dynatmoce.2004.10.015.
Secretariat, C., 2009. Regional Plan of Action: Coral Triangle Initiative on Coral Reefs, Fisheries and Food Security (CTI-CFF), Mondano.
Simons, R.D., Siegel, D.A., Brown, K.S., 2013. Model sensitivity and robustness in the estimation of larval transport: a study of particle tracking parameters, J. Mar. Syst. 119-120(C), 19–29, http://doi.org/10.1016/j.jmarsys.2013.03.004.
Smith, T.M., Reynolds, R.W., Peterson, T.C., Lawrimore, J., 2008. Improvements to NOAA's historical merged land-ocean surface temperature analysis (1880–2006). J. Clim. 21 (10), 2283–2296. http://dx.doi.org/10.1175/2007JCLI2100.1.
Snyder, R.E., Paris, C.B., Vaz, A.C., 2015. How much do marine connectivity fluctuations matter? Am. Natural. 184 (4), 523–530. http://dx.doi.org/10.1086/677925.
Sprintall, J., Révelard, A., 2014. The Indonesian Throughflow response to Indo-Pacific climate variability. J. Geophys. Res. Oceans 119 (2), 1161–1175. http://dx.doi.org/10.1002/2013JC009533.
Sprintall, J., Wijffels, S.E., Molcard, R., Jaya, I., 2009. Direct estimates of the Indonesian Throughflow entering the Indian Ocean: 2004–2006. J. Geophys. Res.: Atmos. 114 (C7), C07001. http://dx.doi.org/10.1029/2008JC005257.
Sudek, M., Aeby, G.S., Davy, S.K., 2011. Localized bleaching in Hawaii causes tissue loss and a reduction in the number of gametes in < Emphasis Type = "Italic" > Porites compressa < /Emphasis > Coral Reefs 31 (2), 351–355. http://dx.doi.org/10.1007/s00338-011-0844-1.
Szmant, A.M., Meadows, M.G., 2006. Developmental changes in coral larval buoyancy and vertical swimming behavior: implications for dispersal and connectivity, In: Proceedings of the 10th International Coral Reef Symposium, vol. 1, pp. 431–437.
Tay, Y.C., Guest, J.R., Chou, L.M., Todd, P.A., 2011. Vertical distribution and settlement competencies in broadcast spawning coral larvae: implications for dispersal models. J. Exp. Mar. Biol. Ecol. 409 (1–2), 324–330. http://dx.doi.org/10.1016/j.jembe.2011.09.013.
Tay, Y.C., Todd, P.A., Rosshaug, P.S., Chou, L.M., 2012. Simulating the transport of broadcast coral larvae among the Southern Islands of Singapore. Aquat. Biol. 15 (3), 283–297. http://dx.doi.org/10.3354/ab00433.
Treml, E.A., Halpin, P.N., 2012. Marine population connectivity identifies ecological neighbors for conservation planning in the Coral Triangle. Conserv. Lett. 5 (6), 441–449. http://dx.doi.org/10.1111/j.1755-263X.2012.00260.x.
Treml, E.A., Roberts, J., Halpin, P.N., Possingham, H.P., Riginos, C., 2015. The emergent geography of biophysical dispersal barriers across the Indo-West Pacific, edited by R. Cowie. Divers. Distrib. 21 (4), 465–476. http://dx.doi.org/10.1111/ddi.12307.
Treml, E.A., Halpin, P.N., Urban, D.L., Pratson, L.F., 2008. Modeling population connectivity by ocean currents, a graph-theoretic approach for marine conservation. Landscape Ecol. 23 (1), 19–36. http://dx.doi.org/10.1007/s10980-007-9138-y.
Van Woesik, R., 2009. Calm before the spawn: global coral spawning patterns are explained by regional wind fields, Proc. R. Soc. Lond. B: Biol. Sci. 277(1682), rspb20091524–722, http://doi.org/10.1098/rspb.2009.1524.
Veron, J.E.N., E. T. A. L. G. S. K. M. S.-S., Devantier, Lyndon M., Peterson, N., 2009. Delineating the Coral Triangle, Galaxea, J. Coral Reef Stud., 1–10.
Wainwright, L., Meyers, G., Wijffels, S., Pigot, L., 2008. Change in the Indonesian Throughflow with the climatic shift of 1976/77. Geophys. Res. Lett. 35 (3), L02606. http://dx.doi.org/10.1029/2007GL031911.
Wallace, C.C., Willis, B.L., 2003. In: Systematics of the Coral Genus Acropora: Implications of New Biological Findings for Species Concepts, http://dx.doi.org/10.1146/annurev.es.25.110194.001321, 25(1), 237-262, doi:10.1146/annurev.es.25.110194.001321.
Wallace, C.C., Richards, Z., 2001. Regional distribution patterns of Acropora and their use in the conservation of coral reefs in Indonesia. Dietriech G. Bengen 40.
Walton, A., et al., 2014. Establishing a functional region-wide coral triangle marine protected area system. Coast. Manage. 42 (2), 107–127. http://dx.doi.org/10.1080/08920753.2014.877765.
Watson, J.R., Kendall, B.E., Siegel, D.A., Mitarai, S., 2012. Changing seascapes, stochastic connectivity, and marine metapopulation dynamics. Am. Natural. 180 (1), 99–112. http://dx.doi.org/10.1086/665992.
Watson, J.R., Mitarai, S., Siegel, D.A., Caselle, J.E., Dong, C., McWilliams, J.C., 2010. Realized and potential larval connectivity in the Southern California Bight. Mar. Ecol. Prog. Ser. 401, 31–48. http://dx.doi.org/10.3354/meps08376.
White, A.T., et al., 2014. Marine protected areas in the coral triangle: progress, issues, and options. Coast. Manage. 42 (2), 87–106. http://dx.doi.org/10.1080/08920753.2014.878177.
Willis, B.L., Babcock R.C., Harrison, P.L., Oliver, J.K., Wallace, C.C., 1985. Patterns in the Mass Spawning of Corals on the Great Barrier Reef from 1981 to 1984.
Wood, S., Paris, C.B., Ridgwell, A., Hendy, E.J., 2014. Modelling dispersal and connectivity of broadcast spawning corals at the global scale. Glob. Ecol. Biogeogr. 23 (1), 1–11. http://dx.doi.org/10.1111/geb.12101.
Wood, S., Baums, I.B., Paris, C.B., Ridgwell, A., Kessler, W.S., Hendy, E.J., 2016. El Niño and coral larval dispersal across the eastern Pacific marine barrier. Nat. Commun. 7, 12571. http://dx.doi.org/10.1038/ncomms12571.
Wyrtki, K., 1961. Physical Oceanography of the Southeast Asian waters, Scripps Institution of Oceanography.
Zang, Y., Wallace, J.M., Battisti, D.S., 1997. ENSO-like interdecadal variability: 1900–1993, 10(5), 1004–1020.